Makes caterpillars floppy-like effector-containing MARTX toxins require host ADP-ribosylation factor (ARF) proteins for systemic pathogenicity

Youngjin Lee[a,1], Byoung Sik Kim[a,b,1], Sanghyeon Choi[a], Eun-Young Lee[a], Shinhye Park[a,c], Jungwon Hwang[a], Yumi Kwon[d,e,f], Jaekyung Hyun[g], Cheolju Lee[d,h,i], Jihyun F. Kim[c], Soo Hyun Eom[j], and Myung Hee Kim[a,2]

[a]Infection and Immunity Research Laboratory, Metabolic Regulation Research Center, Korea Research Institute of Bioscience and Biotechnology, Daejeon 34141, Korea; [b]Department of Food Science and Engineering, Ewha Womans University, Seoul 03760, Korea; [c]Division of Life Sciences, Department of Systems Biology, Yonsei University, Seoul 03722, Korea; [d]Center for Theragnosis, Biomedical Research Institute, Korea Institute of Science and Technology, Seoul 02792, Korea; [e]Department of Life Science, Hanyang University, Seoul 04763, Korea; [f]Research Institute for Natural Sciences, Hanyang University, Seoul 04763, Korea; [g]Electron Microscopy Research Center, Korea Basic Science Institute, Chungcheongbuk-do 28119, Korea; [h]Division of Bio-Medical Science & Technology, Korea University of Science and Technology, Seoul 02792, Korea; [i]Department of Converging Science and Technology, Kyung Hee University - Korea Institute of Science and Technology, Seoul 02447, Korea; and [j]School of Life Sciences, Gwangju Institute of Science and Technology, Gwangju 61005, Korea

Edited by Jorge E. Galán, Yale University School of Medicine, New Haven, CT, and approved July 30, 2019 (received for review March 26, 2019)

Upon invading target cells, multifunctional autoprocessing repeats-in-toxin (MARTX) toxins secreted by bacterial pathogens release their disease-related modularly structured effector domains. However, it is unclear how a diverse repertoire of effector domains within these toxins are processed and activated. Here, we report that Makes caterpillars floppy-like effector (MCF)-containing MARTX toxins require ubiquitous ADP-ribosylation factor (ARF) proteins for processing and activation of intermediate effector modules, which localize in different subcellular compartments following limited processing of holo effector modules by the internal cysteine protease. Effector domains structured tandemly with MCF in intermediate modules become disengaged and fully activated by MCF, which aggressively interacts with ARF proteins present at the same location as intermediate modules and is converted allosterically into a catalytically competent protease. MCF-mediated effector processing leads ultimately to severe virulence in mice via an MCF-mediated ARF switching mechanism across subcellular compartments. This work provides insight into how bacteria take advantage of host systems to induce systemic pathogenicity.

MARTX toxin | effector | ADP-ribosylation factor protein

Bacterial pathogens have the ability to deliver "effector" proteins into host cells to dysregulate a multitude of cell functions, thereby causing severe disease (1). In addition to the typical effector transfer systems, known as type III (2, 3) and IV (4, 5) secretion systems, many gram-negative pathogenic bacteria, which in general lack these typical secretion systems (for example, the sepsis-causing human pathogen *Vibrio vulnificus*), utilize distinct effector transfer machineries, namely, multifunctional autoprocessing repeats-in-toxin (MARTX) toxins (6). These toxins, which are present across multiple bacterial genera (7), are large proteins composed of ∼3,500 to 5,300 amino acid residues that make up 4 distinct regions: the N-terminal repeat domain, the modularly structured multieffector-containing domain, the cysteine protease domain (CPD), and the C-terminal repeat domain (8).

MARTX toxins contribute to lethal effects upon infection. For example, the toxin secreted by clinical isolate *V. vulnificus* CMCP6 (together with the hemolysin VvhA) causes intestinal tissue damage and inflammation, which promote dissemination of infectious bacteria to the bloodstream and other organs (9). Deletion of the toxin gene (*rtxA1*) from another clinical isolate, *V. vulnificus* MO6-24/O, renders it defective with respect to invading the blood stream, resulting in a >100-fold increase in both intragastric and intraperitoneal median lethal dose values in mice (10); this indicates that MARTX toxins are the most significant virulence factor expressed by *V. vulnificus* strains.

Once secreted, MARTX toxins translocate to host cells and undergo an event that releases functionally discrete effector domains in the cytosol (11). The repeat domain regions are proposed to form a pore-like structure that allows the central effector module region to autotranslocate across host cell membranes, although it is not clear how the repeat domains form the pore structure (11–13). Since its discovery, it has been believed that the internal CPD present in all MARTX toxins exclusively directs proteolytic processing of effector modules following its activation and autoprocessing, which are triggered by binding to cytosolic inositol hexakisphosphate ($InsP_6$): This mechanism primes virulence (8, 11, 14–16).

Since homologous recombination events in bacteria bestow variations on the effector content of MARTX toxins, the toxins deliver

Significance

MARTX toxins present across multiple bacterial genera are primary virulence factors that facilitate initial colonization, dissemination, and lethality in a wide range of hosts, including humans. Upon entry into host cells, the toxins undergo a processing event to release their disease-related modularly structured effector domains. However, the mechanisms underlying processing and activation of diverse effector domains within the toxins remain unclear. Here, we use biochemical and structural biological approaches, in combination with cellular microbiological experiments, to demonstrate how Makes caterpillars floppy-like effector (MCF) or its homolog-containing MARTX toxins process effector modules and fully activate effectors. MCF-containing toxins target ADP-ribosylation factor proteins ubiquitously expressed in cells to activate and disseminate effectors across subcellular compartments simultaneously, eventually leading to systemic pathogenicity.

Author contributions: Y.L., B.S.K., and M.H.K. designed research; Y.L., B.S.K., S.C., E.-Y.L., S.P., J. Hwang, Y.K., J. Hyun, and C.L. performed research; S.H.E. contributed new reagents/analytic tools; Y.L., B.S.K., S.C., E.-Y.L., S.P., J. Hwang, Y.K., J. Hyun, C.L., J.F.K., and M.H.K. analyzed data; and Y.L., B.S.K., and M.H.K. wrote the paper.

The authors declare no conflict of interest.

This article is a PNAS Direct Submission.

Data deposition: The atomic coordinates and structure factors have been deposited in the Protein Data Bank, www.wwpdb.org (PDB ID codes 6IMP, 6II0, 6II2, and 6II6).

[1]Y.L. and B.S.K. contributed equally to this work.

[2]To whom correspondence may be addressed. Email: mhk8n@kribb.re.kr.

This article contains supporting information online at www.pnas.org/lookup/suppl/doi:10.1073/pnas.1905095116/-/DCSupplemental.

Published online August 19, 2019.

a diverse repertoire of effector modules into host cells (8, 17, 18). The effector diversity correlates with distinct cytopathicities or cytotoxicities and with the overall toxicity of MARTX toxins (8, 13). At the same time, this diversity suggests that a CPD-dependent strategy may not be the only mechanism that processes and activates effector modules. Indeed, the mechanisms underlying processing and activation of diverse effector domains within the toxins remain unclear.

Here, we show that Makes caterpillars floppy-like effector (MCF) or its homolog-containing MARTX toxins (which comprise approximately one-third of MARTX toxins) are fully activated by a processing mechanism distinct from that which activates solely CPD-containing toxins (approximately two-thirds of MARTX toxins). We found that MCF-containing toxins first undergo limited processing by the CPD, which yields intermediate effector modules (tandemly structured effector-MCF modules). The MCF within the intermediate modules, which localize in different subcellular compartments following CPD-mediated processing, highjacks ADP-ribosylation factor (ARF) proteins present in corresponding subcellular compartments; this leads to further processing and release of fully activated partner effectors via its ARF-mediated allosteric activation into a catalytically competent protease.

Results

MCF-Containing MARTX Toxins Require ARF Proteins to Process Effector Modules into Functional Units. Since the discovery of MARTX toxins, the CPD located in the C-terminal region of effector modules in all MARTX toxins has been thought to be the only processer that releases effectors (8, 11, 14–16). However, we hypothesized that CPD alone may not be sufficient to process the diverse repertoire of effector domains within MARTX toxins to yield functional units. Consequently, we examined CPD-mediated processing using effector domain modules purified from MARTX toxins expressed by 3 different clinical isolates of *V. vulnificus* (MO6-24/O, FORC_009, and BAA87), all of which harbor distinct effector domain repertoires (*SI Appendix*, Fig. S1*A*). Amino acid sequence analysis identified at least 1 putative CPD cleavage site (X_1-L-X_2; where X_1 and X_2 are small amino acids such as Ala and Ser, respectively) (19) in the linker regions between effector domains (*SI Appendix*, Fig. S1*B*). As previously reported (16, 20), CPDs from the MO6-24/O and FORC_009 strains are N-terminally autoprocessed into active forms (aCPDs) by the allosteric activator $InsP_6$; these aCPDs then process effector modules in their cognate MARTX toxins (Fig. 1 *A* and *B*). Notably, effector products generated by the aCPDs were not completely processed into single effector domains. The MARTX toxin harboring 4 effector domains from the MO6-24/O strain was processed into 2 products, DUF1/RID (b in Fig. 1*A*) and ABH/MCF (c in Fig. 1*A*) pairs, indicating that aCPD can only cleave between the RID and ABH domains of this toxin in vitro. In the case of the FORC_009 MARTX toxin, aCPD cleaved between the first MCF and ABH domains and between the second MCF and RRSP domains (Fig. 1*B*). Unexpectedly, the CPD from the BAA87 strain did not process its associated effector domains, even though it was autoprocessed in the presence of $InsP_6$ (Fig. 1*C*).

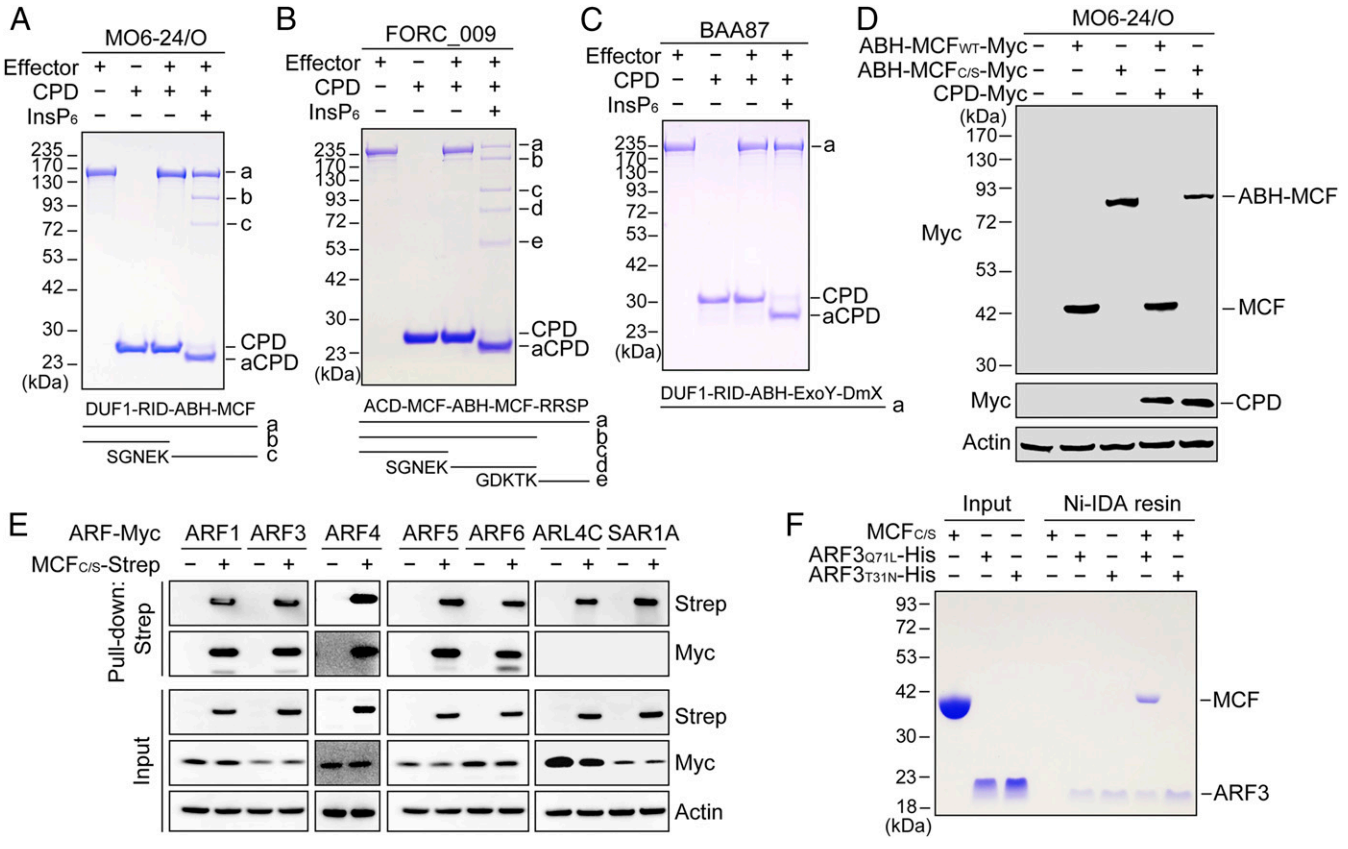

Fig. 1. MARTX toxins undergo a bilateral procedure to process effector modules. (*A*–*C*) Effector modules of *V. vulnificus* MARTX toxins are not completely processed by CPD. Processed products confirmed by Edman sequencing are shown at the bottom of the gels. aCPD, autoprocessed CPD. (*D*) The ABH–MCF pair was processed in cells in a CPD-independent manner. The indicated constructs were coexpressed in HEK293T cells and subjected to Western blotting. (*E*) Pull-down assays showing that MCF interactions are specific for ARF proteins, but not ARF-like proteins. ARL4C, ARF-like protein 4C; SAR1A, secretion-associated Ras-related GTPase 1A. (*F*) In vitro pull-down assay showing that MCF interacts with the active form $ARF3_{Q71L}$, but not with the inactive form $ARF3_{T31N}$. Data are representative of at least 3 independent experiments, each with similar results (*A*–*F*).

Next, we assessed CPD-mediated processing in HEK293T cells; the results showed that the RID/ABH, MCF/ABH, and MCF/RRSP pairs were cleaved by coexpressed cognate CPDs (*SI Appendix*, Fig. S1 *C–E*). This is consistent with the in vitro results (Fig. 1 *A* and *B*). However, unlike in vitro, the effector domain pairs ABH/MCF and ACD/MCF were processed in both the absence and presence of CPD in cells (Fig. 1*D* and *SI Appendix*, Fig. S1*F*). The functional consequence of a free ACD domain is formation of covalently cross-linked actin oligomers (21), which was observed under both conditions (*SI Appendix*, Fig. S1*F*). However, the effector pair harboring a mutation at the MCF catalytic residue ($MCF_{C/S}$) (22) was not cleaved under either condition (Fig. 1*D*), suggesting that processing of the effector pairs is independent of CPD, and that the enzymatic activity of MCF may be responsible for processing together with unknown cellular factor(s). Nonetheless, effector pairs DUF1/RID and ABH/ExoY were not processed in CPD-expressing HEK293T cells (*SI Appendix*, Fig. S1 *G* and *H*), which is consistent with the in vitro results (Fig. 1 *A* and *C*). Therefore, it is unlikely that additional cellular factors are required for the processing of these effector domains, suggesting that these effector pairs may function together in host cells. Collectively, these results suggest that MARTX toxins undergo a bilateral procedure to process effector modules through involvement of both CPD and, possibly, MCF.

The results indicate that effector domains tandemly bound to MCF (i.e., effector-MCF) in MARTX toxins in cells are processed independently of CPD (Fig. 1*D* and *SI Appendix*, Fig. S1*F*). A previous study shows that ectopic expression of *V. vulnificus* MCF in HeLa cells leads to N-terminal autoprocessing in the presence of unidentified cellular factors (22). These observations led us to hypothesize that MARTX toxins harboring MCF may be processed by mechanisms different from those that process only CPD-dependent toxins. Subsequently, we identified potential $MCF_{C/S}$-interacting cellular proteins by affinity purification mass spectrometry. Strikingly, all human ARF proteins (ARF1, ARF3, ARF4, ARF5, and ARF6) were identified as MCF interactors (*SI Appendix*, Fig. S1*I* and Table S1). Pull-down assays subsequently confirmed the mass spectrometry results; all ARF proteins were shown to interact with $MCF_{C/S}$ in HEK293T cells (Fig. 1*E*). However, other ARF-like proteins, namely ARL4C and SAR1A, did not interact with the MCF, suggesting that the MCF interaction is specific for ARF proteins. We further evaluated the interactions at the protein level using His tag pull-down assays with purified proteins, and the results showed that MCF directly interacts with the active form of $ARF3_{Q71L}$, but not with inactive $ARF3_{T31N}$ (Fig. 1*F*).

Next, we asked whether ARF proteins function as cellular factors that activate MCF-mediated processing of intermediate effector modules generated from CPD-mediated processing of holo effector modules. Purified wild-type ABH/MCF_{WT} and mutant $ABH/MCF_{C/S}$ (intermediate modules) were incubated with either active $ARF3_{Q71L}$ or inactive $ARF3_{T31N}$. The results revealed that ABH/MCF_{WT}, but not $ABH/MCF_{C/S}$, was processed into free ABH and MCF by active $ARF3_{Q71L}$ (Fig. 2*A*). The active form of ARF1 and ARF6 also induced MCF-mediated processing (Fig. 2*B*); however, no processing was observed with the active form

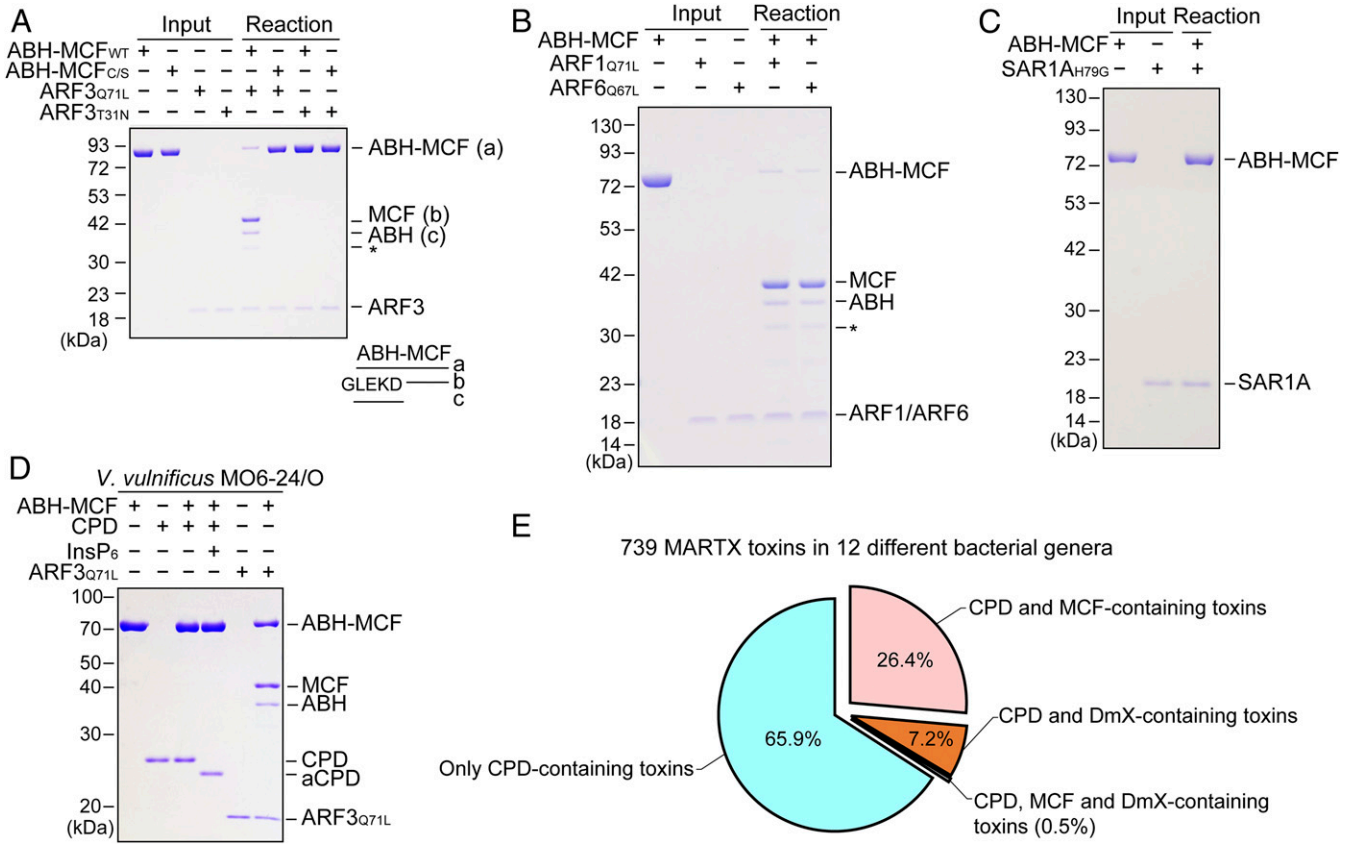

Fig. 2. Host ADP ribosylation factors are essential for processing MCF-containing MARTX toxins from a broad range of pathogenic bacteria. (*A*) Active form ARF is the cellular activator of MCF-mediated processing of the ABH/MCF pair. (*B* and *C*) ARF protein-specific MCF activation and effector pair processing. Processing of the purified ABH/MCF pair was examined using active forms of ARF ($ARF1_{Q71L}$ and $ARF6_{Q67L}$) (*B*) and ARF-like protein $SAR1A_{H79G}$ (*C*). (*D*) ARF-activated MCF processing, not the CPD-mediated processing, is responsible for the ABH/MCF pair processing. (*E*) More than 34% of MARTX toxins contain at least 1 MCF (or its homolog, DmX) domain. Asterisks indicate nonspecific products generated by in vitro cleavage. Data are representative of at least 3 independent experiments, each with similar results (*A–D*).

of ARF-like protein SAR1A (Fig. 2*C*), further supporting the specificity of ARF proteins for MCF activation.

To explore whether ARF-activated MCF processing is common among bacterial pathogens harboring MARTX toxins, we tested effector pairs ABH/MCF, ACD/MCF, and RRSP/MCF of MARTX toxins from different pathogens (*SI Appendix*, Fig. S2*A*). The results clearly showed that these effector pairs are not processed by aCPDs; rather, they are completely processed into free effectors in the presence of active ARF3 (Fig. 2*D* and *SI Appendix*, Fig. S2 *B–F*). This suggests that this processing is common to MCF-harboring MARTX toxins.

The MARTX toxin from the outbreak-associated *V. vulnificus* BAA87 strain (23) harbors distinct effector domains, including ExoY and DmX (*SI Appendix*, Fig. S1*A*). Interestingly, our results showed that its own CPD does not process the effector domains, even though the N-terminal autoprocessing of the CPD occurs in the presence of $InsP_6$ (Fig. 1*C*). This may indicate reduced toxin potency, resulting in decreased virulence of this strain (24). DmX was identified as a cysteine protease that interacts with Golgi-associated ARF proteins 1, 3, and 4 to autoprocess its N terminus for cytopathicity (25). We speculated that DmX may be the enzyme responsible for processing of this toxin. It was clear that the ExoY/DmX pair was processed by active ARF3, suggesting that DmX may be a homolog of MCF (*SI Appendix*, Figs. S2*G* and S3).

The internal CPD-containing MO6-24/O effector module was further purified to examine the activity of the CPD *in cis*. Consistent with its activity *in trans* (Figs. 1*A* and 2*D*), the result showed that CPD is not sufficient for full processing of the effector module and that secondary processing via ARF-activated MCF is required (*SI Appendix*, Fig. S4*A*).

We further analyzed the processing mechanism using MARTX toxin secreted naturally from the MO6-24/O strain. The secreted toxin, a typical fragmented toxin as reported previously (10, 26), was used for processing analysis. Western blot analysis with an anti-ABH antibody showed that the $InsP_6$-activated internal CPD cleaves between RID and ABH to yield intermediate effector module ABH-MCF (*SI Appendix*, Fig. S4 *B–D*). When treated with both $InsP_6$ and the active form of $ARF3_{Q71L}$, the toxin was further processed by the ABH-MCF intermediate module to yield ABH. Note that we observed reaction intermediate product DUF1-RID-ABH, which was confirmed by Edman sequencing.

Taken together, these results support our proposal that MCF or its homolog-containing MARTX toxins from a broad range of pathogenic bacteria require ARF-activated MCF-mediated processing to completely release effectors. Notably, amino acid sequence analysis of 739 MARTX toxins from 12 different bacterial genera revealed that about 34.1% of MARTX toxins possess MCF (26.4%) or an ortholog such as DmX (7.2%), while 65.9% possess only a CPD (Fig. 2*E*).

ARF Is an Allosteric Activator That Converts MCF into a Catalytically Competent Cysteine Protease. Isothermal titration calorimetry (ITC) analysis demonstrated high-affinity interaction between $MCF_{C/S}$ and $ARF3_{Q71L}$, and between intermediate module ABH/$MCF_{C/S}$ and $ARF3_{Q71L}$, with fitting to a 1:1 binding model, yielding dissociation constant (K_d) values of 3.79 nM and 2.19 nM, respectively (Fig. 3*A* and *SI Appendix*, Fig. S5 *A* and *B*). It is worth noting that the cytosolic allosteric activator $InsP_6$ binds to CPD with a K_d of 1.3 μM (16), an affinity ∼500-fold lower than that observed for the ARF and MCF interaction; this suggests that interaction between MCF and ARF proteins may occur overwhelmingly in cells.

To examine the molecular basis of toxin processing mediated by ARF-activated MCF, we next determined the structures of the intermediate effector module ABH/$MCF_{C/S}$ and the $MCF_{C/S}$ and $ARF3_{Q71L}$ complex at resolutions of 3.50 Å and 2.10 Å, respectively (Fig. 3 *B–D* and *SI Appendix*, Fig. S5 *C* and *D* and Table S2). Note that we used catalytically inactive $MCF_{C/S}$ and an active mimic form of $ARF3_{Q71L}$ to minimize conformational variation during both ITC analysis and crystallization.

The structure of tandemly arranged ABH and $MCF_{C/S}$ (hereafter referred to as MCF_A), which represents an intermediate effector module resulting from CPD-mediated processing of MARTX toxins in cells, shows that the effector domains are connected by an α-helical linker containing the MCF autocleavage site (K3218/G3219) (22) (Fig. 3*C*). In the structure, the effector domains interact with each other through the β1 strand and the α5 helix of MCF and the α10 helix of ABH. However, in vitro pull-down assays showed no direct interaction between the effectors (*SI Appendix*, Fig. S5*F*), suggesting that the interaction within the structure may be an artifact of crystal packing. ABH consists of a typical α/β-hydrolase fold spanning residues Ser2927–Asn3205 plus a long N-terminal loop (Glu2909–Leu2926; Fig. 3*C*). Note that ABH does not interact with ARF3 (*SI Appendix*, Fig. S5*G*). Since this study focuses on the MCF-mediated processing of MARTX toxins, we focused mainly on MCF structures.

MCF comprises an N-terminal helix bundle domain (Gly3219–Arg3350; due to its functionality, hereafter this domain will be referred to as switch domain [SD], discussed below) and a C-terminal α/β-fold catalytic domain (CD; Cys3351Ser–Met3565). The MCF CD is folded into an antiparallel 7-stranded β-sheet ordered 1–6–5–4–3–7–2, with α-helices packing on both sides of the β-sheet (Fig. 3*C* and *SI Appendix*, Fig. S5*C*). A structural homology search using the Dali server (27) identified structural similarity between the MCF CD and the α/β-fold of the CPDs (Z-score >5.9), including *Pseudomonas syringae* AvrPphB (Protein Data Bank [PDB] ID code 1UKF), the ubiquitin-specific protease domain of murine cytomegalovirus tegument protein M48 (PDB ID code 2J7Q), and *Shigella flexneri* OspI (PDB ID code 3B21), although these proteins share relatively low sequence identity (11.5 to 14.0%) with MCF (*SI Appendix*, Figs. S3 and S5*H*).

The structure of $MCF_{C/S}$ (hereafter referred to as MCF_B) in the complex with $ARF3_{Q71L}$, which implies ARF-induced MCF activation in cells, shows an arrangement similar to that of the structure of ABH and MCF (Fig. 3 *C* and *D*). Structural comparison with cysteine protease family proteins facilitated assignment of the catalytic triad of MCF, consisting of Cys3351 (a catalytic nucleophile), His3463 (a base that deprotonates and activates the nucleophile), and Asp3482 (an acid that stabilizes the base) that are essential for enzymatic function (Fig. 3*E* and *SI Appendix*, Fig. S5 *I* and *J*). When either of the catalytic residues was mutated, MCF completely lost autocleavage activity in HEK293T cells (Fig. 3*F*). Additionally, superimposition of the active sites of protease structures revealed that Gln3336 may function as an oxyanion residue in MCF (Fig. 3*E* and *SI Appendix*, Fig. S5 *I* and *J*). Consistently, mutation of Gln3336 impaired the catalytic efficiency of MCF in cells (Fig. 3*F*).

MCF_B engages in tight interface interactions with ARF3, principally via the interswitch and Switch 2 regions (Fig. 3*D* and *SI Appendix*, Fig. S6 *A–C*). The ARF3 Switch 2 region (Gly69–Gln86) forms multiple interactions with residues on α4, α5, α7, and 3_{10} helices, and the C-terminal loop of MCF. The interswitch (β2 and β3) is involved in the interaction with α4 of MCF. The interaction network comprises 25 residues in MCF and 22 residues in ARF3. The residues stabilize the tight complex via formation of 5 salt bridges, 16 hydrogen bonds (including 12 water molecules), and 150 hydrophobic contacts (*SI Appendix*, Fig. S6*D*). Both in vitro and in cells, mutation (MCF_{4MT}) of the most critical residues (E3310L, R3317L, Y3381E, and E3397G) completely blocked the interaction between MCF and ARF3

A

	n	K_A (10^8 M^{-1})	K_D (nM)	ΔH (kcal mol^{-1})	TΔS (kcal mol^{-1})	ΔG (kcal mol^{-1})
$ARF3_{Q71L}$ to $MCF_{C/S}$	1.13 ± 0.002	2.64 ± 0.65	3.79	−27.49	−15.97	−11.52
$ARF3_{Q71L}$ to ABH-$MCF_{C/S}$	1.13 ± 0.002	4.57 ± 1.79	2.19	−27.29	−15.47	−11.82

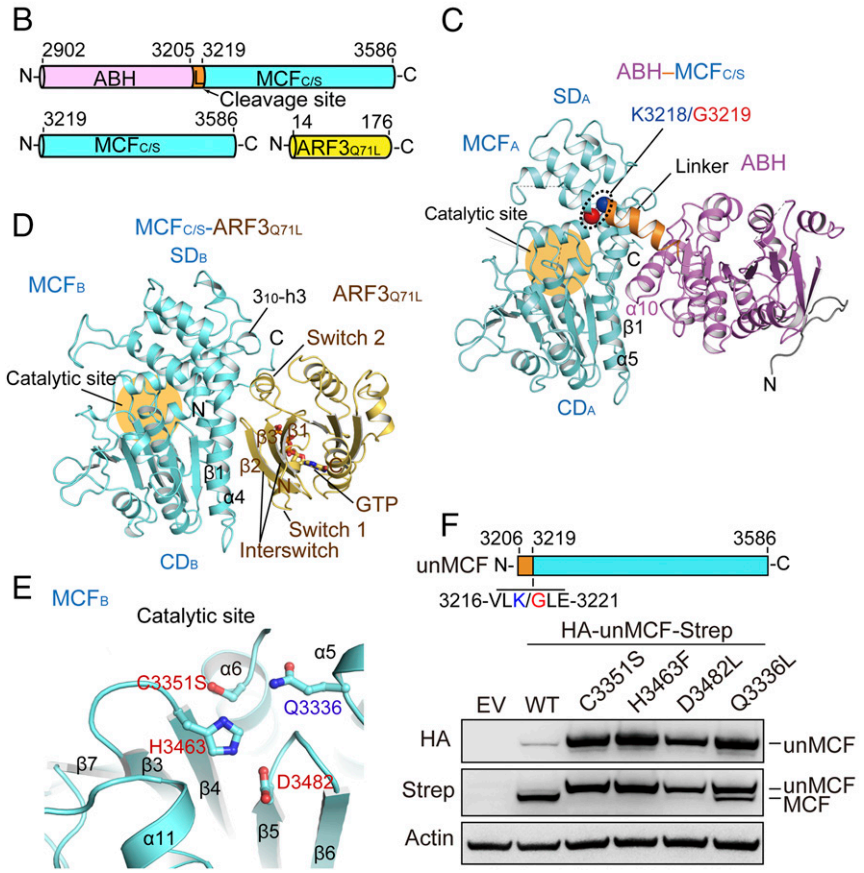

Fig. 3. Crystal structures of $MCF_{C/S}$ either in tandem arrangement with ABH or in complex with $ARF3_{Q71L}$. (*A*) ITC analysis showing a high-affinity interaction between MCF and ARF. (*B*) Schematic diagram of the ABH/MCF pair (residues 2902–3586), MCF (residues 3219–3586), and ARF3 (residues 14–176) used for the structural studies. L, linker connecting ABH and MCF. (*C* and *D*) Overall structures of ABH/$MCF_{C/S}$ (*C*) and the $MCF_{C/S}$–$ARF3_{Q71L}$ complex (*D*). GTP bound to ARF3 is shown as a yellow stick representation (*D*). (*E*) Catalytic site within the $MCF_{C/S}$–$ARF3_{Q71L}$ complex. (*F*) Essential roles of catalytic residues during N-terminal autoprocessing of MCF. The indicated uncleaved MCF constructs (residues 3206–3586) were transiently expressed in HEK293T cells and subjected to Western blotting. EV, empty vector. Data are representative of at least 2 (*A*) or 3 (*F*) independent experiments, each with similar results.

(Fig. 4*A*) and abolished processing of the ABH/MCF intermediate module (Fig. 4 *B* and *C*).

Upon interaction with ARF3, MCF undergoes remarkable conformational changes, particularly in its SD (Fig. 4 *D* and *E*). A significant movement (~10 Å) of the α4 helix in MCF SD_A results in the integration of helix α5 into a long helix α4 in MCF SD_B. This change subsequently causes a large movement (~14 Å) of the other α-helices in SD_B toward the CD. Notably, the disordered region (residues 3335–3350; dark dashed line and L7 loop) in the MCF_A structure (Fig. 4*D*) is dramatically reorganized into an L7 loop, a stable α5 helix, and an L8 loop (an L7-α5-L8 motif; Fig. 4*E*) through numerous hydrophobic contacts between residues of the L7-α5-L8 motif and adjacent hydrophobic residues on α2, α4, α7, α8, and 3_{10}-h1 helices (*SI Appendix*, Fig. S6*E*). One notable feature of this structural reorganization is the relocation of the oxyanion residue Gln3336 from a position far away from the active site in MCF_A into the active site near the catalytic triad residue Cys3351 (Fig. 4 *D*–*F* and *SI Appendix*, Fig. S6*F*). The α5 helix is forced to lean backward, which opens the active site of MCF_B to allow access to the cleavage region between ABH and MCF (Fig. 4*E*). These structural changes and interactions cause movement of the α4, α6–α11, and 3_{10}-h3 helices in CD toward the central antiparallel β-sheet to within 0.7 to 2.1 Å (*SI Appendix*, Fig. S6*G*) and ultimately place the catalytic residues Cys3351, His3463, and Asp3482 into active positions (Fig. 4 *D*–*F*). Collectively, these results demonstrate that ARF is an allosteric activator that converts inactive MCF within intermediate effector modules into a catalytically competent cysteine protease.

ARF Is Essential for Full Activation of Effectors Tandemly Paired with MCF. To gain structural insight into the interaction between intermediate effector module ABH and MCF and ARF in solution, we conducted transmission electron microscopy (TEM) single-particle analysis of negatively stained complexes (*SI Appendix*, Fig. S7 *A*–*F*). TEM analysis of the $MCF_{C/S}$–$ARF3_{Q71L}$ complex revealed well-aligned 2D class averages (*SI Appendix*, Fig. S7 *A* and *B*). Docking the crystal structure of the $MCF_{C/S}$–$ARF3_{Q71L}$ complex onto the TEM 3D reconstruction (23.1-Å

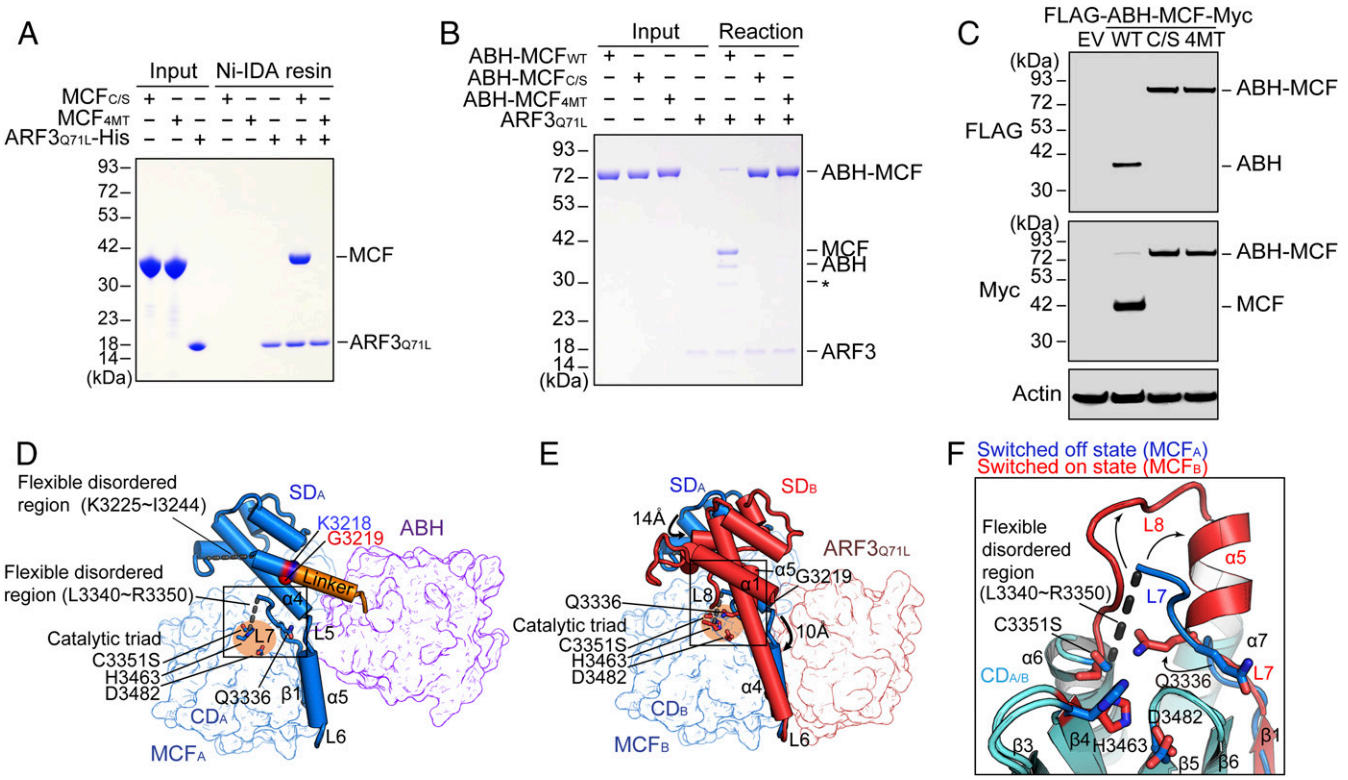

Fig. 4. Molecular basis of ARF-mediated MCF activation. (*A*–*C*) The MCF mutant (MCF_{4MT}, mutated at the positions of E3310L, R3317L, Y3381E, and E3397G) does not interact with ARF. ARF-induced effector processing both in vitro (*B*) and in vivo (*C*). (*D*–*F*) Molecular mechanism underlying ARF-induced allosteric activation of MCF. Inactive MCF_A in ABH/MCF (*D*) is converted into a catalytically competent cysteine protease, MCF_B, upon ARF binding (*E*). Expanded view of the catalytic and oxyanion residues within each structure (*F*). Data are representative of 3 independent experiments, each with similar results (*A*–*C*).

resolution, as determined by the 0.5 criteria of the Fourier shell correlation [FSC] curve; *SI Appendix*, Fig. S7*G*) showed good overall agreement in terms of the organization of MCF and ARF3 (*SI Appendix*, Fig. S7*H*). By contrast, particle images of the negatively stained ABH/$MCF_{C/S}$ intermediate module were poorly aligned when 2D class averaging was attempted, although particles of a size compatible with the effectors (~10 nm in the longest dimension) were discernible from the class averages (*SI Appendix*, Fig. S7 *C* and *D*), suggesting that tandemly structured ABH and MCF is dynamic, possibly due to the flexible interdomain linker.

TEM analysis of the negatively stained ABH/$MCF_{C/S}$–$ARF3_{Q71L}$ complex revealed well-distributed, homogeneous particles (*SI Appendix*, Fig. S7 *E* and *F*). However, the particle sizes and shapes observed in 2D class averaging were incompatible with the ternary complex; rather, they were similar to those observed after class averaging of the $MCF_{C/S}$–$ARF3_{Q71L}$ complex (*SI Appendix*, Fig. S7 *B* and *F*). Based on the observation that $MCF_{C/S}$–$ARF3_{Q71L}$ remains structurally intact, whereas ABH/$MCF_{C/S}$ is highly flexible, the class averages should reflect a stable $MCF_{C/S}$–$ARF3_{Q71L}$ complex while loosely/flexibly bound ABH should be averaged out during image processing. The 3D reconstruction (24.5-Å resolution, as determined by the 0.5 criteria of the FSC curve; *SI Appendix*, Fig. S7*G*) of the ternary complex exhibited major density similar to that of $MCF_{C/S}$–$ARF3_{Q71L}$, but with apparent additional "noise" proximal to the MCF SD (*SI Appendix*, Fig. S7*I*). In an attempt to segregate different conformations of the ternary complex, particles extracted from the consensus 3D reconstruction were classified into four 3D classes without orientation alignment (*SI Appendix*, Fig. S7*J*). Although the resulting maps were noisy and could not identify discrete positions for the additional density, it was clear that this extra density remained close to the MCF SD, suggesting that this position may accommodate flexibly bound ABH via the linker region (*SI Appendix*, Fig. S7*K*). Following the continuous density at the N terminus of MCF, ABH appears to reside directly above $MCF_{C/S}$–$ARF3_{Q71L}$ rather than being associated laterally; therefore, it is likely to lift the flexible linker loop away from MCF to facilitate insertion of the cleavage sequence-containing loop into the active site (*SI Appendix*, Fig. S7*K*). Thus, these results suggest that the helical linker between ABH and $MCF_{C/S}$ in the crystal structure is likely to be a fully or partially unfolded loop in the tandemly structured intermediate effector module, rather than a stable helix. In addition, these results imply that effectors tandemly structured with MCF are fully exposed upon interaction with ARF.

To evaluate the effect of ARF on effectors tandemly structured with MCF, we performed ACD-mediated actin cross-linking assays using HeLa cells infected with a series of engineered strains that produce a MARTX toxin harboring 2 domains (ACD/MCF_{WT}, ACD/$MCF_{C/S}$, and ACD/MCF_{4MT}; Fig. 5*C*). A mutant strain producing an effector-free MARTX toxin (EF-MARTX) was used as a negative control (Fig. 5*A*). The strain harboring ACD paired with $MCF_{C/S}$ (a processing-defective mutant with ARF interaction ability) revealed actin cross-linking activity, albeit significantly reduced compared with that of the strain harboring ACD paired with MCF_{WT}. The strain harboring ACD paired with MCF_{4MT} (an ARF interaction-defective mutant) displayed considerably less actin cross-linking activity (Fig. 5 *B* and *C*), supporting our hypothesis that ARF may induce exposure of effectors upon interaction with MCF (*SI Appendix*, Fig. S7*K*). Thus, these results strongly suggest that the ARF interaction with MCF is essential not only for MCF activation, but also for full activation of effectors tandemly paired with MCF.

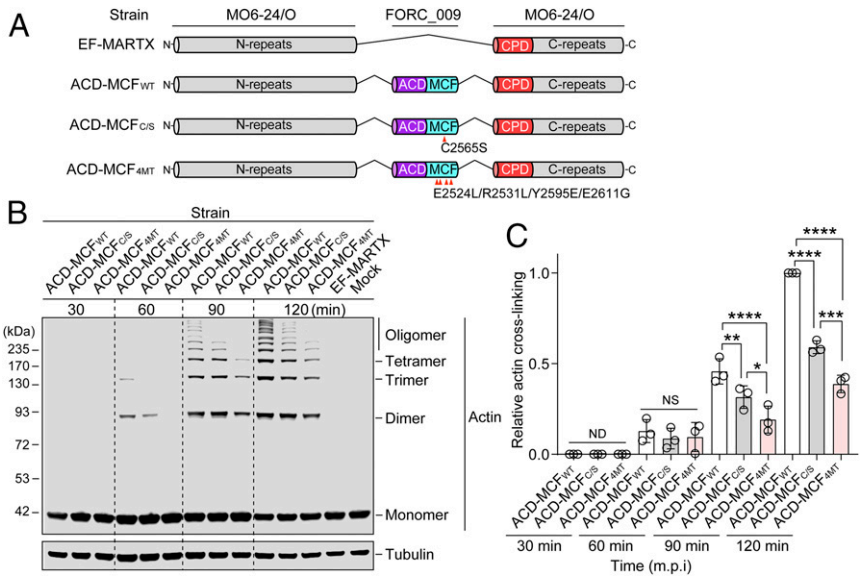

Fig. 5. ARF binding to MCF is essential for full activation of tandemly paired effectors. (*A*) Schematic representation of modified MARTX toxins in the engineered strains. Mutated positions in MCF are indicated. (*B* and *C*) Actin in HeLa cells infected with the indicated strains was analyzed by Western blotting (*B*). Band intensities were quantified, and levels of actin cross-linking relative to those in ACD/MCF$_{WT}$ were calculated and presented (*C*). Data are expressed as the mean ± SD of biological triplicates (****$P < 0.0001$; ***$P < 0.001$; **$P < 0.01$; *$P < 0.05$; NS, not significant; ND, not detected).

MCF Switches Interacting ARF Proteins in Cells for Systemic Pathogenicity. Interactome analysis (*SI Appendix*, Fig. S1*I*), along with pull-down (Fig. 1*E*) and in vitro processing (Fig. 2 *A* and *B*) assays, revealed that MCF may interact with all human ARF proteins, implying that MCF may switch interacting ARF proteins in cells. Human ARF proteins share high amino acid sequence identity, and the residues responsible for interaction with MCF are highly conserved (*SI Appendix*, Fig. S8*A*). Thus, the binding affinity for MCF may be similar, meaning that competitive interaction between ARF proteins and MCF would not occur. Rather, a cellular factor such as ARF GTPase-activating protein (ARFGAP) may be involved in dissociation of ARF from MCF prior to switching ARF. Therefore, we examined ARFGAP1, which inactivates all human ARF proteins by stimulating GTP hydrolysis (28, 29). Indeed, it appeared to dissociate ARF3 from MCF in HEK293T cells (*SI Appendix*, Fig. S8*B*). Furthermore, mutation of Arg50 in ARFGAP1, which is essential for its activity, had little effect on the interaction between the 2 proteins (*SI Appendix*, Fig. S8*C*), suggesting that ARFGAP may be the cellular factor involved in dissociation of ARF from MCF.

To further explore the consequences of dissociating MCF from ARF, we determined the structure of free MCF$_{C/S}$ (hereafter referred to as MCF$_C$) at a resolution of 2.36 Å (Fig. 6*A* and *SI Appendix*, Fig. S5*E* and Table S2). Superimposition of MCF$_C$ onto MCF$_B$ reveals a large conformational change in the SD, but no significant change in CD (Fig. 6*B* and *SI Appendix*, Fig. S8*D*). The long α4 helix, α5, and β1 in the MCF–ARF3 complex are dramatically rotated (~101°) away from the CD. This large movement blocks the active site and converts α5 in MCF$_B$ to β2 in MCF$_C$, thereby moving oxyanion residue Gln3336 away from the active site (Figs. 4*E* and 6*B* and *SI Appendix*, Fig. S8*D*). Accordingly, the rest of the N-terminal helices in the SD are rotated in the same direction by ~82° in MCF$_C$. Since the catalytic triad in the catalytic site of MCF$_C$ remains identical to that in the active form in MCF$_B$, we evaluated whether free MCF remains functional. In vitro assays showed that free MCF had no enzymatic activity (*SI Appendix*, Fig. S8*E*), further confirming that ARF binding is required to maintain MCF in an active conformation.

To assess whether ARF switching by MCF occurs in cells, we used catalytically inactive ABH$_{S/A}$ to generate a series of ABH/MCF constructs C-terminally fused with green fluorescent protein (GFP) (30); this enabled us to focus on MCF function. C-terminally GFP-fused ABH$_{S/A}$ localized at the plasma membrane in HEK293T cells (*SI Appendix*, Fig. S9*A*), whereas C-terminally GFP-fused MCF is expressed in the cytoplasm (22). When ectopically expressed in HEK293T cells, ABH$_{S/A}$/MCF$_{4MT}$ and ABH$_{S/A}$/MCF$_{C/S}$ effector pairs localized predominantly at the plasma membrane, indicating that the CPD-driven ABH/MCF intermediate is first localized to the plasma membrane in an ABH-dependent manner (Fig. 6*C*). However, GFP signals were evenly distributed in both the cytoplasm and perinucleus of cells expressing ABH$_{S/A}$/MCF$_{WT}$ (Fig. 6*C*), suggesting that plasma membrane-localized ARF (e.g., ARF6) processes the intermediate effector module at the plasma membrane (31), followed by release of MCF-GFP into the cytoplasm and perinucleus where ARF1/3 resides (29). Confocal microscopy revealed that ABH$_{S/A}$/MCF$_{C/S}$ colocalizes with ARF6 in the plasma membrane, whereas localization of ABH$_{S/A}$/MCF$_{4MT}$ and ARF6 differs somewhat (Fig. 6*C*). ABH$_{S/A}$/MCF$_{WT}$ colocalizes with ARF3 particularly in the perinucleus (Fig. 6*C*), supporting our proposal that MCF switches interacting ARF proteins across subcellular compartments in cells.

MCF causes severe cell shrinkage (22), and we observed cell shrinkage only with the ABH$_{S/A}$/MCF$_{WT}$ module but not with ABH$_{S/A}$/MCF$_{4MT}$ or ABH$_{S/A}$/MCF$_{C/S}$ (Fig. 6*C*), indicating that ARF6-induced MCF activation in the plasma membrane is necessary for cytopathic consequences. Thus, these results suggest that initial localization and activation of MCF in cells is dependent on its partner effector, and the type of ARF interacting with MCF is location-dependent.

DmX, a functional homolog of MCF, is N-terminally autoprocessed following binding with Golgi-associated ARF proteins, leading to cytopathicity (25). Since we observed colocalization of MCF and ARF3 in the perinucleus (Fig. 6*C*), we examined Golgi dispersion by staining the *cis*-Golgi marker GM130. Consistent with the morphological changes, Golgi were severely disrupted, and barely detectable in ABH$_{S/A}$/MCF$_{WT}$-expressing cells, but were intact in ABH$_{S/A}$/MCF$_{4MT}$- and ABH$_{S/A}$/MCF$_{C/S}$-expressing

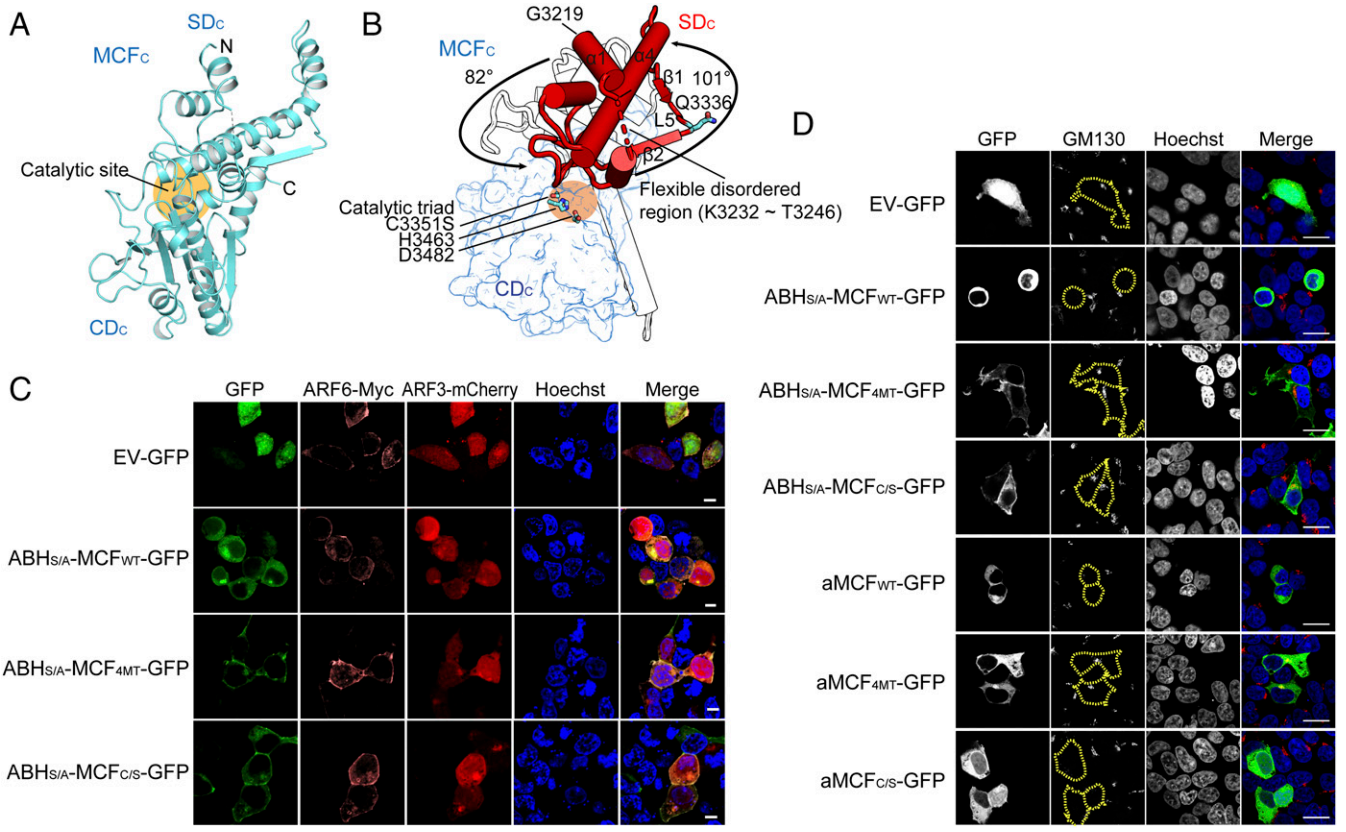

Fig. 6. MCF switches interacting ARF proteins across subcellular compartments. (*A*) Overall structure of free $MCF_{C/S}$. (*B*) Structural significance of inactive $MCF_{C/S}$ released from ARF, showing a large conformational change in the SD (red). The conformation of the SD in active MCF_B complexed with ARF3 is shown by black lines. (*C*) MCF switches interacting ARF proteins in HEK293T cells. (Scale bars, 10 μm.) (*D*) Interaction between MCF and ARF proteins results in Golgi dispersion and cell shrinkage. Before confocal microscopy analysis, the *cis*-Golgi marker GM130 and nuclei were stained. Margins of transfected cells in the GM130 panel are indicated by yellow dashed lines. (Scale bars, 20 μm.) Data are representative of 3 independent experiments, each with similar results (*C* and *D*).

cells (Fig. 6*D*), further supporting the importance of MCF-mediated ARF switching.

To further verify the importance of MCF function, we generated a free form of MCF_{WT} that mimics MCF translocated into the cytoplasm from the plasma membrane and expressed it in HEK293T cells. Cells expressing MCF_{WT} exhibited a shrunken morphology with disrupted Golgi, similar to cells expressing $ABH_{S/A}$/MCF_{WT} (Fig. 6*D*). However, cells expressing the ARF interaction-deficient mutant MCF_{4MT} were not affected in terms of morphology or Golgi, demonstrating that interaction with ARF3, and possibly ARF1, is essential for the cytotoxicity of MCF. Interestingly, the morphology of cells expressing catalytically inactive $MCF_{C/S}$ was unaffected, but Golgi were disrupted (Fig. 6*D*), suggesting that sequestering of ARF proteins by MCF mainly affects the Golgi structure, and that a cellular substrate of MCF linked to cell shrinkage may exist. It should be mentioned that ARF proteins regulate endoplasmic reticulum and Golgi morphology and function (32–35).

To evaluate whether cytopathic or cytotoxic effects are common to all MCF and MCF homologs in different MARTX toxins, we tested MCF (MCF_{Xn}) from the Xenorhabdus *nematophila* (an insect pathogen) MARTX toxin and MCF homolog DmX (DmX_{Pl}) from the *Photorhabdus luminescens* (a lethal pathogen of insects) MARTX toxin (*SI Appendix*, Fig. S9*B*). It is noteworthy that MCF_{Xn} showed ARF-dependent intermediate effector module processing (*SI Appendix*, Fig. S2*F*). When mammalian HEK293T cells were transiently transfected with MCF_{Xn}, the latter localized to the Golgi; however, no cytopathic or cytotoxic effects were observed, suggesting that MCF_{Xn} may not exhibit cytopathic or cytotoxic effects in mammalian hosts. However, it may exert cytopathic or cytotoxic effects by targeting a substrate in its natural host (e.g., insects). Meanwhile, similar to MO6-24/O MCF, the MCF homolog DmX_{Pl} caused shrinkage of HEK293T cells, suggesting that the substrate of DmX_{Pl} may be conserved in both insect and mammalian hosts. Collectively, these results suggest that all MCFs and homologs in different MARTX toxins are functional for toxin processing, but their cytopathic or cytotoxic effects may be different.

To further demonstrate the significance of ARF-mediated MCF function during pathogenesis of *V. vulnificus* in vivo, we engineered a series of mutant strains to produce a MARTX toxin harboring only 2 domains: $ABH_{S/A}$/MCF_{WT}, $ABH_{S/A}$/$MCF_{C/S}$, or $ABH_{S/A}$/MCF_{4MT} (Fig. 7*A*). When female ICR mice were subcutaneously challenged with 5×10^6 colony-forming units of the parental wild-type strain (Parental), all mice succumbed within 10 h postinfection (Fig. 7*B*). By contrast, 60% of mice survived until the end of the experiment when the EF-MARTX strain was used (Fig. 7*B*), demonstrating the significance of MARTX toxin effector domains in the pathogenesis of *V. vulnificus* in vivo, as reported previously (36). Although virulence did not fully recover to levels observed for the parental strain, complementation with functional MCF upon infection with the $ABH_{S/A}$/MCF_{WT} strain resulted in 100% mortality at 10 to 15 h postinfection (Fig. 7*B*; EF-MARTX vs. $ABH_{S/A}$/MCF_{WT}; $P < 0.0001$). By comparison, 50% and 30% of mice infected with the $ABH_{S/A}$/$MCF_{C/S}$ and $ABH_{S/A}$/MCF_{4MT} strains, respectively, survived until the end of the experiments, which is comparable to the survival rate after infection with the EF-MARTX strain (Fig. 7*B*, $P = 0.4346$ and 0.0695, respectively). Collectively, these results indicate that

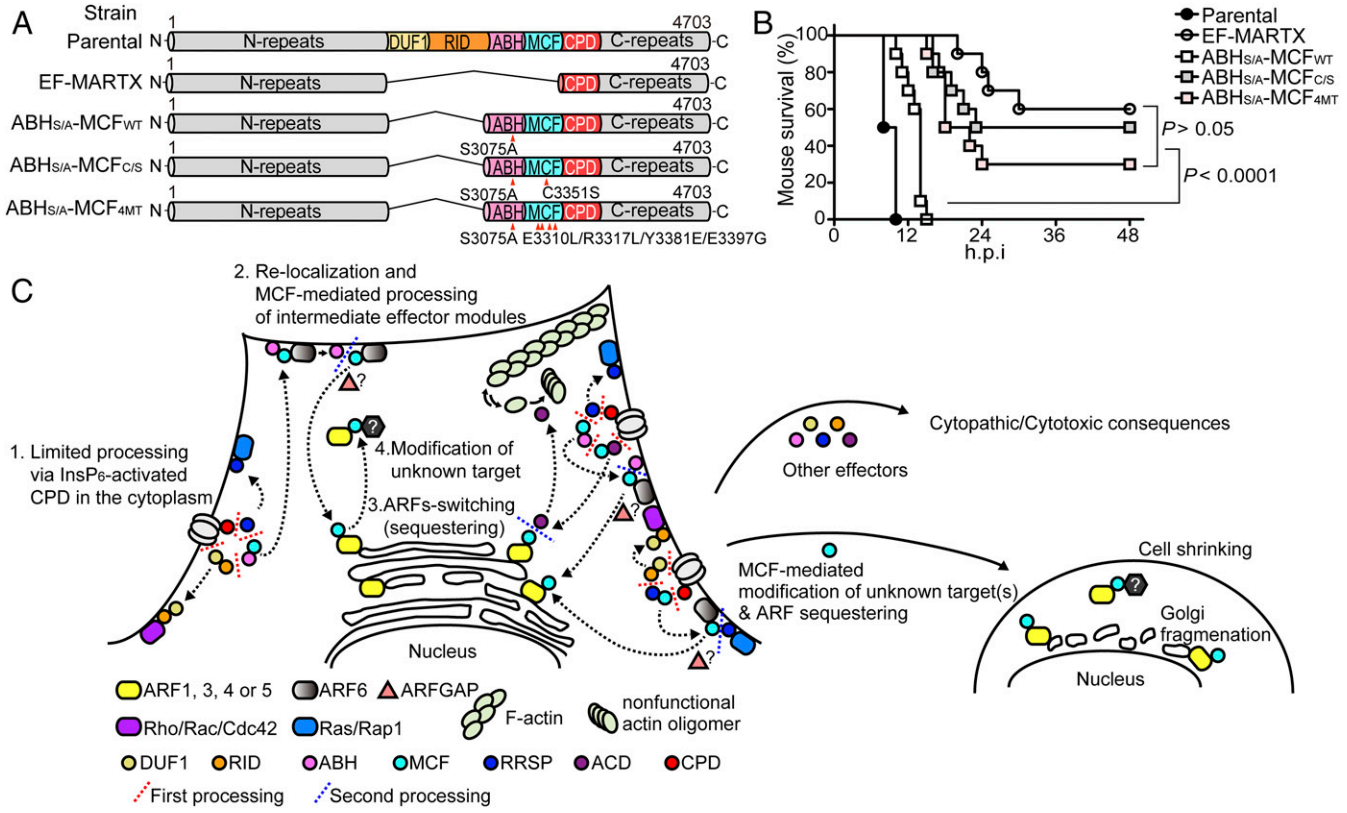

Fig. 7. Significance of processing and activation of MCF-containing MARTX toxins. (*A*) Schematic representation of modified MARTX toxins in the engineered strains. Mutated positions are indicated. (*B*) Survival of mice ($n = 10$ per group; pooled data from 2 experiments) challenged subcutaneously with the engineered strains, illustrating the significance of MCF interactions with ARF proteins. (*C*) Proposed model showing processing and activation of MCF-containing MARTX toxins. After translocation, MARTX effector domains are first processed by CPD in the cytoplasm, resulting in tandemly arranged effector-MCF intermediate modules as well as free single effector(s). The effector intermediate (ABH/MCF) relocalizes to the plasma membrane, where MCF interacts with and is activated by ARF6, followed by a second round of processing. ARFGAP-mediated inactivation of ARF6 may release MCF into the cytoplasm, which subsequently sequesters other ARF proteins and/or modifies unknown cellular substrate(s). Other intermediate effector modules tandemly paired with MCF may undergo similar processing events. As a result, MCF causes Golgi fragmentation and cell shrinkage, while other effectors have cytopathic/cytotoxic consequences.

MCF-mediated ARF switching is critical for MARTX toxin-mediated virulence of pathogens.

Discussion

Here, we show that MCF or its homolog-containing MARTX toxins undergo a series of distinct processing procedures to fully activate effectors within the toxins, leading to systemic pathogenicity. These procedures include limited processing via $InsP_6$-activated CPD in the cytoplasm, relocalization of intermediate effector modules to different subcellular compartments, MCF-mediated processing of these intermediate modules induced by ubiquitous ARF proteins to fully activate partner effectors, and MCF-mediated switching of ARF proteins (possibly via ARFGAP) (Fig. 7*C*).

About 10 effector domains have been identified in different MARTX toxins (37). These effectors localize to different subcellular compartments to function: For example, ABH (*SI Appendix*, Fig. S9*A*) and RRSP (38, 39) localize to the plasma membrane and ACD localizes in the cytoplasm (40). Although we demonstrated ARF-activated MCF-mediated processing using the intermediate ABH and MCF modules, we can speculate that effectors tandemly structured with MCF from different MARTX toxins would be fully activated by the same processing mechanism, thereby conferring pathogenicity (Fig. 7*C*).

Amino acid sequence analysis of MARTX toxins from 12 bacterial genera showed that about one-third of the toxins possess MCF or an ortholog such as DmX (Fig. 2*E*). In terms of pathogenic efficacy, cytosolic $InsP_6$-dependent CPD alone may not be sufficient for processing different types of effectors localized within different subcellular compartments, suggesting that bacteria may evolve to overcome this limitation and expand their virulence via domain addition (e.g., MCF or its homolog), perhaps via homologous recombination events. Evolution is highly sophisticated and targets ARF proteins ubiquitously expressed in cells, taking advantage of host systems to activate and disseminate virulence-related partner effectors across subcellular compartments simultaneously. By doing so, an MCF-mediated processing strategy can guarantee the coordinated functions of simultaneously delivered effector domains, which are crucial for the overall outcome of MARTX toxins (13). Furthermore, this distinctive strategy allows bacteria to ensure MARTX toxin processing, even in the presence of nonfunctional CPD, as observed for the *V. vulnificus* BAA87 strain (Fig. 1*C* and *SI Appendix*, Fig. S2*G*). Future studies should examine whether acquisition of MCF correlates with the severity of infection by pathogenic bacteria.

We demonstrated that ARF activates MCF allosterically to yield a catalytically competent cysteine protease. We extensively analyzed the autocleavage sequence of MCF (between partner effectors and itself) within all MARTX toxins and found that MCF recognizes consensus sequences "X_1-L-K-G-X_2," where L, K, and G are strictly conserved and X_1 and X_2 are small and

bulky hydrophobic amino acids; MCF then cleaves between Lys and Gly (*SI Appendix*, Fig. S9*C*). $InsP_6$-activated CPD cleaves "X_1-L-X_2" (where X_1 and X_2 are small amino acids) in the linker regions between effector domains within MARTX toxins, as well as within its own N-terminal region (autocleavage) (19). With respect to sequence recognition, it seems that MCF has more stringent substrate specificity than CPD. We suggested that ARF-activated MCF has a cellular substrate in the cytoplasm, which is responsible for cell shrinking (Fig. 6*D*). The MCF-recognizing consensus sequences may provide hints that will enable us to identify the cellular substrate.

ARF proteins are utilized by microbial invaders to facilitate their dissemination and virulence via different host mechanisms (41–50). The results presented herein suggest that ARF proteins are allosteric activators that are aggressively exploited by bacterial pathogens to increase virulence. This unique strategy developed by pathogens may be a promising target for antitoxin therapeutics.

Materials and Methods

See *SI Appendix* for details of the strains, cells, mice, protein purification, in vitro processing assays, Edman sequencing, effector processing in cells, pull-down assays, Western blotting, ITC, in vitro pull-down assays, crystallization, X-ray diffraction data collection and structure determination, structural analysis, TEM and image processing, confocal microscopy, liquid chromatography-tandem mass spectrometry analysis, strain engineering, actin cross-linking assay, and mouse survival tests. Statistical analysis was performed using GraphPad Prism 7. Significance was determined by Tukey's multiple comparison tests after 2-way analysis of variance. For the mouse survival tests, statistical significance was determined using the Mantel–Cox log-rank test.

The Institutional Animal Care and Use Committee of the Korea Research Institute of Bioscience and Biotechnology approved all mouse experiment protocols (approval no. KRIBB-AEC-18186).

ACKNOWLEDGMENTS. We thank beamline staff at the Pohang Accelerator Laboratory (BL-5C and 7A), Korea, and the Photon Factory (BL-17A), Japan, for assistance during X-ray diffraction experiments. We thank all members of the M.H.K. laboratory for valuable discussion and technical support. This work was supported by the National Research Foundation of Korea, funded by the Ministry of Science and ICT of Korea (2014R1A2A1A01005971 and 2017R1A2B3007317 to M.H.K. and 2018R1C1B5045632 to B.S.K.), the Korea Research Institute of Bioscience and Biotechnology Initiative Program, and a grant from Korea Health Industry Development Institute (HI14C3484 to C.L.).

1. J. E. Galán, Common themes in the design and function of bacterial effectors. *Cell Host Microbe* **5**, 571–579 (2009).
2. T. P. Moest, S. Méresse, Salmonella T3SSs: Successful mission of the secret(ion) agents. *Curr. Opin. Microbiol.* **16**, 38–44 (2013).
3. J. E. Galán, H. Wolf-Watz, Protein delivery into eukaryotic cells by type III secretion machines. *Nature* **444**, 567–573 (2006).
4. E. C. So, C. Mattheis, E. W. Tate, G. Frankel, G. N. Schroeder, Creating a customized intracellular niche: Subversion of host cell signaling by *Legionella* type IV secretion system effectors. *Can. J. Microbiol.* **61**, 617–635 (2015).
5. R. Fronzes *et al*., Structure of a type IV secretion system core complex. *Science* **323**, 266–268 (2009).
6. K. L. Sheahan, C. L. Cordero, K. J. Satchell, Autoprocessing of the *Vibrio cholerae* RTX toxin by the cysteine protease domain. *EMBO J.* **26**, 2552–2561 (2007).
7. B. S. Kim, The modes of action of MARTX toxin effector domains. *Toxins (Basel)* **10**, E507 (2018).
8. K. J. Satchell, Structure and function of MARTX toxins and other large repetitive RTX proteins. *Annu. Rev. Microbiol.* **65**, 71–90 (2011).
9. H. G. Jeong, K. J. Satchell, Additive function of *Vibrio vulnificus* MARTX(Vv) and VvhA cytolysins promotes rapid growth and epithelial tissue necrosis during intestinal infection. *PLoS Pathog.* **8**, e1002581 (2012).
10. Y. R. Kim *et al*., *Vibrio vulnificus* RTX toxin kills host cells only after contact of the bacteria with host cells. *Cell Microbiol.* **10**, 848–862 (2008).
11. A. Shen, Autoproteolytic activation of bacterial toxins. *Toxins (Basel)* **2**, 963–977 (2010).
12. B. S. Kim, H. E. Gavin, K. J. Satchell, Distinct roles of the repeat-containing regions and effector domains of the *Vibrio vulnificus* multifunctional-autoprocessing repeats-in-toxin (MARTX) toxin. *MBio* **6**, e00324-15 (2015).
13. P. J. Woida, K. J. F. Satchell, Coordinated delivery and function of bacterial MARTX toxin effectors. *Mol. Microbiol.* **107**, 133–141 (2018).
14. M. Egerer, K. J. Satchell, Inositol hexakisphosphate-induced autoprocessing of large bacterial protein toxins. *PLoS Pathog.* **6**, e1000942 (2010).
15. K. Prochazkova *et al*., Structural and molecular mechanism for autoprocessing of MARTX toxin of *Vibrio cholerae* at multiple sites. *J. Biol. Chem.* **284**, 26557–26568 (2009).
16. P. J. Lupardus, A. Shen, M. Bogyo, K. C. Garcia, Small molecule-induced allosteric activation of the *Vibrio cholerae* RTX cysteine protease domain. *Science* **322**, 265–268 (2008).
17. K. J. Satchell, MARTX, multifunctional autoprocessing repeats-in-toxin toxins. *Infect. Immun.* **75**, 5079–5084 (2007).
18. F. J. Roig, F. González-Candelas, C. Amaro, Domain organization and evolution of multifunctional autoprocessing repeats-in-toxin (MARTX) toxin in *Vibrio vulnificus*. *Appl. Environ. Microbiol.* **77**, 657–668 (2011).
19. A. Shen *et al*., Mechanistic and structural insights into the proteolytic activation of *Vibrio cholerae* MARTX toxin. *Nat. Chem. Biol.* **5**, 469–478 (2009).
20. K. Prochazkova, K. J. Satchell, Structure-function analysis of inositol hexakisphosphate-induced autoprocessing of the *Vibrio cholerae* multifunctional autoprocessing RTX toxin. *J. Biol. Chem.* **283**, 23656–23664 (2008).
21. K. L. Sheahan, C. L. Cordero, K. J. Satchell, Identification of a domain within the multifunctional *Vibrio cholerae* RTX toxin that covalently cross-links actin. *Proc. Natl. Acad. Sci. U.S.A.* **101**, 9798–9803 (2004).
22. S. Agarwal, S. Agarwal, M. Biancucci, K. J. Satchell, Induced autoprocessing of the cytopathic makes caterpillars floppy-like effector domain of the *Vibrio vulnificus* MARTX toxin. *Cell Microbiol.* **17**, 1494–1509 (2015).
23. N. Bisharat *et al*.; Israel Vibrio Study Group, Clinical, epidemiological, and microbiological features of *Vibrio vulnificus* biogroup 3 causing outbreaks of wound infection and bacteraemia in Israel. *Lancet* **354**, 1421–1424 (1999).
24. B. S. Kim, H. E. Gavin, K. J. F. Satchell, Variable virulence of biotype 3 *Vibrio vulnificus* due to MARTX toxin effector domain composition. *MSphere* **2**, e00272-17 (2017).
25. B. S. Kim, K. J. Satchell, MARTX effector cross kingdom activation by Golgi-associated ADP-ribosylation factors. *Cell Microbiol.* **18**, 1078–1093 (2016).
26. J. H. Lee *et al*., Identification and characterization of the *Vibrio vulnificus rtxA* essential for cytotoxicity in vitro and virulence in mice. *J. Microbiol.* **45**, 146–152 (2007).
27. L. Holm, C. Sander, Protein structure comparison by alignment of distance matrices. *J. Mol. Biol.* **233**, 123–138 (1993).
28. M. Bai *et al*., ARFGAP1 promotes AP-2-dependent endocytosis. *Nat. Cell Biol.* **13**, 559–567 (2011).
29. J. G. Donaldson, C. L. Jackson, ARF family G proteins and their regulators: Roles in membrane transport, development and disease. *Nat. Rev. Mol. Cell Biol.* **12**, 362–375 (2011).
30. S. Agarwal *et al*., Autophagy and endosomal trafficking inhibition by *Vibrio cholerae* MARTX toxin phosphatidylinositol-3-phosphate-specific phospholipase A1 activity. *Nat. Commun.* **6**, 8745 (2015). Erratum in: *Nat. Commun*. **6**, 10135 (2015).
31. M. M. Cavenagh *et al*., Intracellular distribution of Arf proteins in mammalian cells. Arf6 is uniquely localized to the plasma membrane. *J. Biol. Chem.* **271**, 21767–21774 (1996).
32. C. Dascher, W. E. Balch, Dominant inhibitory mutants of ARF1 block endoplasmic reticulum to Golgi transport and trigger disassembly of the Golgi apparatus. *J. Biol. Chem.* **269**, 1437–1448 (1994).
33. C. J. Zhang *et al*., Expression of a dominant allele of human ARF1 inhibits membrane traffic in vivo. *J. Cell Biol.* **124**, 289–300 (1994).
34. P. Melançon *et al*., Involvement of GTP-binding "G" proteins in transport through the Golgi stack. *Cell* **51**, 1053–1062 (1987).
35. T. C. Taylor, R. A. Kahn, P. Melançon, Two distinct members of the ADP-ribosylation factor family of GTP-binding proteins regulate cell-free intra-Golgi transport. *Cell* **70**, 69–79 (1992).
36. H. E. Gavin, N. T. Beubier, K. J. Satchell, The effector domain region of the *Vibrio vulnificus* MARTX toxin confers biphasic epithelial barrier disruption and is essential for systemic spread from the intestine. *PLoS Pathog.* **13**, e1006119 (2017).
37. H. E. Gavin, K. J. Satchell, MARTX toxins as effector delivery platforms. *Pathog. Dis.* **73**, ftv092 (2015).
38. S. Y. Jang *et al*., Structural basis of inactivation of Ras and Rap1 small GTPases by Ras/Rap1-specific endopeptidase from the sepsis-causing pathogen *Vibrio vulnificus*. *J. Biol. Chem.* **293**, 18110–18122 (2018).
39. M. Biancucci *et al*., The bacterial Ras/Rap1 site-specific endopeptidase RRSP cleaves Ras through an atypical mechanism to disrupt Ras-ERK signaling. *Sci. Signal.* **11**, eaat8335 (2018).
40. D. S. Kudryashov *et al*., Connecting actin monomers by iso-peptide bond is a toxicity mechanism of the *Vibrio cholerae* MARTX toxin. *Proc. Natl. Acad. Sci. U.S.A.* **105**, 18537–18542 (2008).
41. M. Kudelko *et al*., Class II ADP-ribosylation factors are required for efficient secretion of dengue viruses. *J. Biol. Chem.* **287**, 767–777 (2012).
42. R. Farhat *et al*., Identification of class II ADP-ribosylation factors as cellular factors required for hepatitis C virus replication. *Cell Microbiol.* **18**, 1121–1133 (2016).
43. G. A. Belov *et al*., Hijacking components of the cellular secretory pathway for replication of poliovirus RNA. *J. Virol.* **81**, 558–567 (2007).
44. A. Dautry-Varsat, A. Subtil, T. Hackstadt, Recent insights into the mechanisms of Chlamydia entry. *Cell Microbiol.* **7**, 1714–1722 (2005).
45. R. S. Goody, A. Itzen, Modulation of small GTPases by *Legionella*. *Curr. Top. Microbiol. Immunol.* **376**, 117–133 (2013).
46. N. Y. Hsu *et al*., Viral reorganization of the secretory pathway generates distinct organelles for RNA replication. *Cell* **141**, 799–811 (2010).
47. D. Humphreys, A. C. Davidson, P. J. Hume, L. E. Makin, V. Koronakis, Arf6 coordinates actin assembly through the WAVE complex, a mechanism usurped by *Salmonella* to invade host cells. *Proc. Natl. Acad. Sci. U.S.A.* **110**, 16880–16885 (2013).
48. M. Matto *et al*., Role for ADP ribosylation factor 1 in the regulation of hepatitis C virus replication. *J. Virol.* **85**, 946–956 (2011).
49. R. A. Kahn, A. G. Gilman, The protein cofactor necessary for ADP-ribosylation of Gs by cholera toxin is itself a GTP binding protein. *J. Biol. Chem.* **261**, 7906–7911 (1986).
50. C. J. O'Neal, M. G. Jobling, R. K. Holmes, W. G. Hol, Structural basis for the activation of cholera toxin by human ARF6-GTP. *Science* **309**, 1093–1096 (2005).